DEUTSCHES ELEKTRONEN-SYNCHROTRON DESY

DESY 87-115
PITHA 87-18
FTUAM-EP-87-07
September 1987

A STUDY OF BHABHA SCATTERING AT PETRA ENERGIES

by

TASSO Collaboration

ISSN 0418-9833

NOTKESTRASSE 85 · 2 HAMBURG 52

DESY 87-115
PITHA 87-18
FTUAM-EP-87-07
September 1987

ISSN 0418-9833

A Study of Bhabha Scattering at PETRA Energies

TASSO Collaboration

September 1987

W. Braunschweig, R. Gerhards, F.J. Kirschfink, H.-U. Martyn, P. Rosskamp
I. Physikalisches Institut der RWTH Aachen, Federal Republic of Germany[a]

B. Bock, H.M. Fischer, H. Hartmann, J. Hartmann, E. Hilger, A. Jocksch, V. Mertens[1], R. Wedemeyer
Physikalisches Institut der Universität Bonn, Federal Republic of Germany[a]

B. Foster, A.J. Martin, A.J. Sephton
H.H. Wills Physics Laboratory, University of Bristol, Bristol, UK[b]

F. Barreiro[11,15], E. Bernardi, J. Chwastowski[2], Y. Eisenberg[3], A. Eskreys[4], K. Gather, K. Genser[5], H. Hultschig, P. Joos, H. Kowalski, A. Ladage, B. Löhr, D. Lüke, P. Mättig[6], A. Montag[3], D. Notz, J. Pawlak[5], E. Ronat[3], E. Ros, D. Trines, T. Tymieniecka[7], R. Walczak[7], G. Wolf, W. Zeuner
Deutsches Elektronen-Synchrotron DESY, Hamburg, Federal Republic of Germany

H. Kolanoski
Physikalisches Institut, Universität Dortmund, Federal Republic of Germany[a]

T. Kracht, J. Krüger, E. Lohrmann, G. Poelz, K.-U. Pösnecker
II. Institut fur Experimentalphysik der Universität Hamburg, Federal Republic of Germany[a]

D.M. Binnie, J.K. Sedgbeer, J. Shulman, D. Su, A.T. Watson
Dept. of Physics, Imperial College, London, UK[b]

J.P. Cerezo, M.A. Garcia[16], A. Leites, J. del Peso, J.F. de Troconiz
Universidad Autónoma de Madrid, Madrid, Spain[c]

C. Balkwill, M.G. Bowler, P.N. Burrows, R.J. Cashmore, P. Dauncey[8], G.P. Heath, D.J. Mellor[9], P. Ratoff, I. Tomalin, J.M. Yelton
Dept. of Nuclear Physics, Oxford University, Oxford, UK[b]

S.L. Lloyd
Dept. of Physics, Queen Mary College, London, UK[b]

G.E. Forden[10], J.C. Hart, D.H. Saxon
Rutherford Appleton Laboratory, Chilton, Didcot, UK[b]

S. Brandt, M. Holder, L. Labarga[11]
Fachbereich Physik der Universität-Gesamthochschule Siegen, Federal Republic of Germany[a]

U. Karshon, G. Mikenberg, D. Revel, A. Shapira, N. Wainer, G. Yekutieli
Weizmann Institute, Rehovot, Israel[d]

G. Baranko[12], A. Caldwell[13], J.M. Izen[9], D. Muller, S. Ritz, D. Strom, M. Takashima, E. Wicklund[14], Sau Lan Wu, G. Zobernig
Dept. of Physics, University of Wisconsin, Madison, WI, USA[e]

[1] Now at CERN, Geneva, Switzerland
[2] On leave from Inst. of Nuclear Physics, Cracow, Poland
[3] On leave from Weizmann Institute, Rehovot, Israel
[4] Now at Inst. of Nuclear Physics, Cracow, Poland
[5] On leave from Warsaw University, Poland
[6] Now at IPP Canada, Carleton University, Ottowa, Canada
[7] Now at Warsaw University, Poland
[8] Now at Johns Hopkins University, Baltimore, MD, USA
[9] Now at Univ. of Illinois at Urbana-Champaign, Urbana, IL, USA
[10] Now at SUNY Stony Brook, Stony Brook, NY, USA
[11] On leave from Universidad Autónoma de Madrid, Madrid, Spain
[12] Now at University of Colorado, Colorado, USA
[13] Now at Columbia University, New York, USA
[14] Now at California Inst. of Technology, Pasadena, CA, USA
[15] Supported by the Alexander von Humboldt Stiftung
[15] Supported by Cajamadrid
[a] Supported by Bundesministerium für Forschung und Technologie
[b] Supported by UK Science and Engineering Research Council
[c] Supported by CAICYT
[d] Supported by the Minerva Gesellschaft fur Forschung GmbH
[e] Supported by US Dept. of Energy, contract DE-AC02-76ER000881 and by US Nat. Sci. Foundation Grant no INT-8313994 for travel

Abstract

We report on high statistics Bhabha scattering data taken with the TASSO experiment at PETRA at center of mass energies from 12 GeV to 46.8 GeV. We present an analysis in terms of electroweak parameters of the standard model, give limits on QED cut-off parameters and look for possible signs of compositeness.

1 Introduction

Bhabha scattering $e^+e^- \to e^+e^-$ is the most simple purely leptonic reaction to be studied at e^+e^- colliders. It has been used in the past by the TASSO collaboration [1] as well as by other experiments at PETRA and PEP [2] to test QED, its extension to the standard model of electroweak interactions [3], to search for compositeness, and to set limits on the pointlike structure of electrons. This paper reviews all our results obtained at center of mass energies ranging from $\sqrt{s} = 12\,GeV$ up to the highest values of $\sqrt{s} = 46.8\,GeV$ at the PETRA storage ring.

The paper is organized as follows. We first present the relevant cross section formula. Then we briefly discuss the experimental conditions of data taking and analysis. Then follows the determination of electroweak coupling constants. Finally we present limits on QED cut-off parameters and mass scale parameters in composite models. A summary concludes our investigations.

2 Cross section formula

The cross sections were evaluated using the formula of ref. [4] for the electroweak interaction and extended by the authors of [5] for composite models. For unpolarized beams the differential cross section can be written in the following form

$$\frac{d\sigma}{d\Omega} = \frac{\alpha^2}{8\,s} \cdot \left\{ 4\,B_1 + B_2\,(1-\cos\theta)^2 + B_3\,(1+\cos\theta)^2 \right\}\,, \qquad (1)$$

with

$$\begin{aligned}
B_1 &= \left(\frac{s}{t}\right)^2 \left| 1 + (g_V^2 - g_A^2)\,\xi \pm \frac{\eta_{RL}\,t}{\alpha\,\Lambda_\pm^{C\,2}} \right|^2 , \\
B_2 &= \left| 1 + (g_V^2 - g_A^2)\,\chi \pm \frac{\eta_{RL}\,s}{\alpha\,\Lambda_\pm^{C\,2}} \right|^2 , \\
B_3 &= \frac{1}{2} \left| 1 + \frac{s}{t} + (g_V + g_A)^2 \left(\frac{s}{t}\,\xi + \chi\right) \pm \frac{2\,\eta_{RR}\,s}{\alpha\,\Lambda_\pm^{C\,2}} \right|^2 \\
&+ \frac{1}{2} \left| 1 + \frac{s}{t} + (g_V - g_A)^2 \left(\frac{s}{t}\,\xi + \chi\right) \pm \frac{2\,\eta_{LL}\,s}{\alpha\,\Lambda_\pm^{C\,2}} \right|^2 , \\
\chi &= \frac{G_F\,M_Z^2}{2\sqrt{2}\,\pi\,\alpha} \cdot \frac{s}{s - M_Z^2 + iM_Z\Gamma}\,, \\
\xi &= \frac{G_F\,M_Z^2}{2\sqrt{2}\,\pi\,\alpha} \cdot \frac{t}{t - M_Z^2 + iM_Z\Gamma}\,.
\end{aligned}$$

Here α is the fine structure constant, s is the center of mass energy squared, θ is the polar scattering angle measured between the incoming and the outgoing electron, and $t = -\frac{s}{2}(1-\cos\theta)$. In the standard $SU(2)_L \times U(1)$ model the weak contributions are described by the vector coupling $g_V = -\frac{1}{2} + 2\,\sin^2\theta_W$, the axial vector coupling $g_A = -\frac{1}{2}$, the weak mixing angle $\sin^2\theta_W$ and propagator terms given by the Fermi constant G_F, the Z^0 mass M_Z and the Z^0 width Γ. For calculations within the standard model we use $\sin^2\theta_W = 0.23$ and $M_Z = 92\,GeV$ [6]. Note that the chosen parametrization is not sensitive to the exact value of M_Z.

Composite models are tested by allowing some of the coefficients η to be different from zero and the mass scale Λ^C to be finite. The indices R and L denote right handed and left handed currents, respectively.

The pure QED case can be derived by setting g_V, g_A and all η's to zero. Traditionally any departure from QED has been paramatrized by inserting time-like and space-like form factors at the respective vertices with cut-off parameters Λ^{QED}

$$F_T(s) = 1 \mp \frac{s}{s - \Lambda_\pm^{QED\,2}}\,, \qquad (2)$$

$$F_S(t) = 1 \mp \frac{t}{t - \Lambda_\pm^{QED\,2}}\,. \qquad (3)$$

This assumes, however, that any new current couples to the electron with the same strength and transformation properties as the photon field.

3 Event selection

The data were taken from 1979 to 1986 with the TASSO detector at the e^+e^- storage ring PETRA. The energy span reaches from $\sqrt{s} = 12\,GeV$ to $\sqrt{s} = 46.8\,GeV$. Since large parts of the luminosity have been taken during energy scans the data have been grouped at certain average energies, as listed in Table 1.

The TASSO detector, the trigger conditions and the event selection criteria have been described elsewhere [1] and will be only briefly recalled. The trigger required two charged track-candidates having an acoplanarity angle measured in the plane perpendicular to the beam direction of less than 25^0. A charged track candidate at the trigger level was required to have hits in the central proportional chamber, the central drift chamber, the corresponding time-of-flight counter, and for part of the data also in the vertex detector. The trigger and reconstruction efficiencies were checked with data taken concurrently with other independent triggers, e.g. two track triggers with no acoplanarity condition and shower counter triggers. The efficiencies were determined with a typical accuracy of $\pm 1\%$ and, most important, did not show any significant polar angle dependence (the maximum deviation observed for a small fraction of the data was 3% over $\cos\theta = 0$ to $|\cos\theta| = 0.8$).

The Bhabha event analysis is solely based on event topologies, no electron identification was attempted. The selection of two prong events required:

- two opppositely charged tracks,
- an acollinearity angle between the two tracks of $\zeta < 10^0$.
- a polar angle acceptance of $|\cos\theta| < 0.80$ for each track.
- a momentum $p > 0.2 \cdot p_{beam}$ for each track and $\sum p > 0.7 \cdot p_{beam}$ for the sum of both tracks,
- the vertex of both tracks to match the nominal interaction point within 0.6 cm perpendicular to the beam and 7.5 cm along the beam,
- the time-of-flight for each track to be within $-3.0 < t^{meas} - t^{predicted} < 2.0\,ns$.

The background in the thus selected two prong event sample from two photon processes $e^+e^- \to e^+e^- l^+l^-$ and cosmic rays was negligible. The contributions from μ pairs (5% overall and 20% in the backward hemisphere) and τ pairs (1%) were subtracted bin by bin taking the standard model production cross section with our measured charge asymmetries into account [1,7,8]. The charge identification was ensured by our high precision central tracking devices. By studying the correlations of the charge weighted reciprocal momenta of forward versus backward going tracks we found a charge confusion probability per track of 0.3 ± 0.1 % (0.5 ± 0.1 %) at $\sqrt{s} = 35\,GeV$ ($44\,GeV$) and a correlated probability that both tracks flip the charge simultaneously of less than 10^{-5} ($2 \cdot 10^{-5}$) at $\sqrt{s} = 35\,GeV$ ($44\,GeV$). This is consistent with the assumption that both curvature measurements are independent of each other as can be derived from the achieved transverse momentum resolution for high energy tracks of $\sigma(1/p_\perp)/(1/p_\perp) = 0.016$.

4 Experimental results

The acceptance functions to correct the measured angular distributions were calculated using a Monte Carlo program [9]. The showering of electrons and radiating photons was simulated with the EGS code[10]. The simulations were checked with Bhabha events identified by the liquid argon calorimeters and good agreement with the data was found. The overall uncertainty in the bin-to-bin polar acceptance due to shower corrections, trigger and reconstruction efficiencies was estimated to be less than 1% and was added in quadrature to the statistical errors.

The data have also been corrected for QED radiative effects up to order α^3 [9]. Weak radiative corrections have not yet been provided in a form of a Monte Carlo generator program, but are estimated to be negligible at PETRA energies [11].

The overall systematic uncertainty for the luminosity determination from wide angle Bhabha scattering amounted typically to $\pm(3.0 - 3.5)$%. The luminosity measurement as derived from small angle Bhabha scattering had a typical uncertainty of $\pm(3.5 - 4.5)$%. Since both luminosity determinations from wide angle and small angle measurements agree very well and wide angle Bhabha scattering deviates only marginally from QED (see later) we assumed for the extraction of physiscs parameters a conservative systematic overall uncertainty of ±3%. This overall systematic uncertainty is not included in the cross section data points shown in the figures or tables.

The differential cross sections for five average energies at $\sqrt{s} = 14$, 22, 34.8, 38.3 and 43.6 GeV are shown in Fig. 1 and listed in Table 2. A more detailed presentation of the ratio of the measured cross section to the QED expectation on a linear scale is given in Fig. 2. The total cross section integrated over $|\cos\theta| < 0.80$ as function of the energy is displayed in Fig. 3.

5 Determination of electroweak coupling constants

The data shown in Figs. 1 and 2 can be well described either by the QED prediction or by its electroweak extension. In fact a fit of our highest statistics data at $\sqrt{s} = 34.8\,GeV$ to the QED cross section yields a $\chi^2 = 21.8$ for 19 d.o.f., while the standard model prediction yields a slightly better description with $\chi^2 = 20.6$. In all fits an overall normalization factor is considered as a free parameter.

The data can be used to determine the Weinberg angle $\sin^2\theta_W$. A fit of our high energy data (i.e. above 34 GeV) to the standard model yields $\sin^2\theta_W = 0.24 \pm 0.04$ to be compared with the value 0.28 ± 0.12 obtained from a previous analysis at $\sqrt{s} = 34.6\,GeV$ with less statistics [1]. If the absolute normalization is held fixed then the error on the determination of $\sin^2\theta_W$ can be reduced by a factor of two to ±0.02.

We have attempted to measure the square of the vector and axial vector coupling constants in the context of a general SU(2)$\times$U(1) electroweak theory. A fit to our high energy data yields $g_V^2 = -0.08 \pm 0.04$ and $g_A^2 = 0.14 \pm 0.09$. It should be noted, however, that both coupling constants are strongly correlated with a correlation coefficient of 0.5, thus making their simultaneous determination somewhat unreliable. If the vector coupling constant is fixed to zero, a value required by QED and close to the standard model expectation, we obtain for the axial vector coupling $g_A^2 = 0.26 \pm 0.07$, in favour of the standard model.

As discussed in section 2 departures from QED have been traditionally parametrized in terms of cut-off parameters Λ^{QED} introduced in eqs. (2) and (3). Investigating possible departures in the energy dependence of the total cross section data of Fig. 3 we find lower limits (95% confidence level) of $\Lambda_+^{QED} > 370\,GeV$ and $\Lambda_-^{QED} > 190\,GeV$. These bounds can be improved by fitting the differential cross sections after having applied corrections due to the electroweak interference. The corresponding lower limits (95% confidence level) are $\Lambda_+^{QED} > 435\,GeV$ and $\Lambda_-^{QED} > 590\,GeV$. These results can be interpreted that electrons are point-like objects down to distances of $5 \cdot 10^{-17}$ cm.

In Table 3 our results concerning the determination of electroweak coupling constants and QED cut-off parameters are summarized.

6 Test of composite models

In models of compositeness the fundamental fermions are supposed to have a substructure. Bhabha scattering is particularly simple since initial and final state particles are the same and no assumptions on the constituents have to be made. A general parametrization of the interaction at the sub-constituent level can be formulated under the assumption that the standard electroweak theory is correct and one adds to its Lagrangian a contact interaction term of the form

$$\mathcal{L}_{eff} = \pm \frac{g^2}{2\,\Lambda_\pm^{C\,2}} (\eta_{LL}\, j_L\, j_L + \eta_{RR}\, j_R\, j_R + 2\,\eta_{RL}\, j_R\, j_L) \,.$$

The parameter Λ^C characterizes the mass scale of compositeness subject to the condition that $g^2/4\pi = 1$. As usual j_R and j_L denote right handed and left handed currents. The interference between this contact interaction and the γ and Z exchange in the standard theory is responsible for the terms appearing in eq. (1) proportional to the η's. In the present analysis we assumed for simplicity that these constants take the values 0 or ±1. Thus for the LL coupling $\eta_{LL} = 1$, $\eta_{RR} = \eta_{RL} = 0$, for the RR coupling $\eta_{RR} = 1$, $\eta_{LL} = \eta_{RL} = 0$, for the VV coupling $\eta_{LL} = \eta_{RR} = \eta_{RL} = 1$ and for the AA coupling $\eta_{RR} = \eta_{LL} = -\eta_{RL} = 1$. Fitting the high energy Bhabha data to eq. (1) one obtains lower limits for the mass scale parameters Λ^C which are summarized in Table 4. They are typically between 1.4 to 7 TeV, depending on the chiral structure of the currents. LL and RR couplings cannot be distinguished at present energies. The sensitivity of our highest statistics data at $\sqrt{s} = 34.8\,GeV$ to various values of Λ^C is illustrated in Fig. 4.

7 Conclusions

We have presented a high statistics analysis of Bhabha scattering at center of mass energies between 12 and 46.8 GeV. While our data are still consistent with QED, they are better described within the standard electroweak model. Particularly interesting is the determination of $\sin^2\theta_W = 0.24 \pm 0.04$ from a purely leptonic reaction. The determination of electroweak coupling constants, lower limits on QED cut-off paramaters and mass scales of composite models have been considerably improved over previous experiments.

Acknowledgements. We gratefully acknowledge the support by the DESY directorate, the PETRA machine group and the DESY computer center. Those of us from outside DESY wish to thank the DESY directorate for the hospitality extended to us while working at DESY.

References

[1] Tasso Coll., M.Althoff et al., Z. Phys. C22 (1984) 13

[2] Cello Coll., H.-J.Behrend et al., Z. Phys. C16 (1983) 301
Jade Coll., W.Bartel et al., Z. Phys. C19 (1983) 197; B. Naroska, Phys. Rep. 148 (1987) 67
Mark J Coll., B.Adeva et al., MIT-LNS Report 131 (1983)
Pluto Coll., Ch. Berger et al., Z. Phys. C27 (1985) 341
HRS Coll., M. Derrick et al., Phys. Lett. 166B (1986) 463
MAC Coll., E. Fernandez et al., Phys. Rev. D35 (1987) 10

[3] S.L. Glashow, Nucl. Phys. 22 (1961) 579
A. Salam, Proc. eighth Nobel Symp., p.367 (ed.N.Svartholm, Stockholm, Almquist and Wiksell 1968)
S. Weinberg, Phys. Rev. Lett. 19 (1967) 1264

[4] R. Budny, Phys. Lett. 55B (1975) 227

[5] E.J. Eichten, K.D. Lane, M.E. Peskin, Phys. Rev. Lett. 50 (1983) 811

[6] Particle Data Group, Phys. Lett. 170B (1986) 1
U. Amaldi et al.,'A comprehensive analysis of data pertaining to the weak neutral current and intermediate vector boson masses', University of Pennsylvania UPR - 331T (1987)

[7] Tasso Coll., M.Althoff et al., Z. Phys. C26 (1985) 521

[8] H.-U. Martyn, Proc. 22. Rencontre de Moriond, Les Arcs, France, 1987, and Aachen report PITHA 87-09

[9] F.A. Berends, R. Kleiss, Nucl. Phys. B206 (1983) 61

[10] R.L. Ford, W.R. Nelson, EGS Code, SLAC-210 (1978)

[11] M. Böhm, A. Denner, W. Hollik, DESY 86-165 (1986), and W. Hollik private communication

$\langle \sqrt{s} \rangle$ (GeV)	$\int \mathcal{L}\, dt$ (pb^{-1})	N_{Bhabha}
14.0	1.7	10730
22.0	2.7	7106
34.8	174.5	166348
38.3	8.9	6035
43.6	37.1	22951

Table 1: Data samples used for the analysis $e^+e^- \rightarrow e^+e^-$

$\langle\cos\theta\rangle$	$\sqrt{s} = 14.0\,GeV$ $s \cdot d\sigma/d\Omega$ $(nb \cdot GeV^2)$	$\sigma^{meas}/\sigma^{QED}$	$\sqrt{s} = 22.0\,GeV$ $s \cdot d\sigma/d\Omega$ $(nb \cdot GeV^2)$	$\sigma^{meas}/\sigma^{QED}$	$\sqrt{s} = 34.8\,GeV$ $s \cdot d\sigma/d\Omega$ $(nb \cdot GeV^2)$	$\sigma^{meas}/\sigma^{QED}$	$\sqrt{s} = 38.3\,GeV$ $s \cdot d\sigma/d\Omega$ $(nb \cdot GeV^2)$	$\sigma^{meas}/\sigma^{QED}$	$\sqrt{s} = 43.6\,GeV$ $s \cdot d\sigma/d\Omega$ $(nb \cdot GeV^2)$	$\sigma^{meas}/\sigma^{QED}$
0.775	1431.0 ± 29.7	1.063 ± 0.022	1319.0 ± 33.6	0.980 ± 0.025	1336.8 ± 14.7	0.993 ± 0.011	1326.0 ± 36.4	0.985 ± 0.027	1290.0 ± 22.1	0.958 ± 0.016
0.725	907.9 ± 22.5	1.055 ± 0.026	839.3 ± 25.5	0.976 ± 0.029	861.0 ± 9.9	1.001 ± 0.012	893.1 ± 28.4	1.038 ± 0.033	825.1 ± 16.1	0.959 ± 0.019
0.675	603.5 ± 17.9	1.022 ± 0.030	583.7 ± 20.8	0.989 ± 0.035	587.3 ± 7.1	0.995 ± 0.012	576.7 ± 22.8	0.977 ± 0.039	565.5 ± 12.7	0.958 ± 0.022
0.625	435.1 ± 15.1	1.021 ± 0.035	396.3 ± 17.0	0.930 ± 0.040	419.1 ± 5.5	0.984 ± 0.013	408.8 ± 19.2	0.960 ± 0.045	426.9 ± 10.7	1.002 ± 0.025
0.575	330.8 ± 13.1	1.034 ± 0.040	296.1 ± 14.6	0.926 ± 0.046	315.5 ± 4.4	0.987 ± 0.014	312.6 ± 16.7	0.978 ± 0.053	309.9 ± 8.9	0.969 ± 0.028
0.525	241.6 ± 11.2	0.976 ± 0.045	250.0 ± 13.4	1.010 ± 0.054	249.1 ± 3.7	1.007 ± 0.015	249.3 ± 14.9	1.008 ± 0.060	247.4 ± 7.9	1.000 ± 0.032
0.450	182.7 ± 6.9	1.037 ± 0.039	159.5 ± 7.6	0.905 ± 0.043	172.0 ± 2.4	0.976 ± 0.014	181.6 ± 9.1	1.030 ± 0.051	174.1 ± 4.8	0.989 ± 0.027
0.350	122.6 ± 5.6	1.023 ± 0.047	114.1 ± 6.4	0.952 ± 0.053	118.5 ± 1.8	0.989 ± 0.015	114.1 ± 7.1	0.952 ± 0.060	120.7 ± 3.9	1.007 ± 0.033
0.250	84.9 ± 4.8	0.981 ± 0.055	78.1 ± 5.4	0.902 ± 0.062	84.8 ± 1.5	0.980 ± 0.017	85.1 ± 5.9	0.983 ± 0.069	92.7 ± 3.5	1.071 ± 0.040
0.150	63.8 ± 4.2	0.973 ± 0.063	63.1 ± 4.9	0.962 ± 0.074	61.9 ± 1.2	0.943 ± 0.018	65.9 ± 5.4	1.004 ± 0.082	55.2 ± 2.7	0.842 ± 0.041
0.050	55.6 ± 3.9	1.073 ± 0.076	47.2 ± 4.3	0.910 ± 0.082	51.2 ± 1.1	0.988 ± 0.021	49.3 ± 4.8	0.951 ± 0.093	47.3 ± 2.5	0.913 ± 0.049
−0.050	40.7 ± 3.4	0.959 ± 0.080	38.6 ± 3.9	0.910 ± 0.092	42.0 ± 0.9	0.990 ± 0.022	33.0 ± 4.1	0.777 ± 0.096	36.3 ± 2.2	0.856 ± 0.053
−0.150	34.1 ± 3.2	0.953 ± 0.089	35.7 ± 3.8	0.998 ± 0.106	35.4 ± 0.8	0.987 ± 0.024	36.1 ± 4.1	1.008 ± 0.116	36.0 ± 2.2	1.004 ± 0.062
−0.250	34.4 ± 3.2	1.106 ± 0.102	28.6 ± 3.5	0.920 ± 0.111	30.9 ± 0.8	0.993 ± 0.026	28.1 ± 3.7	0.902 ± 0.117	26.9 ± 2.0	0.863 ± 0.063
−0.350	25.0 ± 2.8	0.902 ± 0.102	28.4 ± 3.5	1.023 ± 0.125	26.5 ± 0.7	0.954 ± 0.027	21.0 ± 3.5	0.759 ± 0.125	22.7 ± 1.8	0.819 ± 0.067
−0.450	28.7 ± 3.0	1.136 ± 0.120	25.9 ± 3.4	1.025 ± 0.136	24.7 ± 0.7	0.975 ± 0.029	28.7 ± 4.1	1.134 ± 0.161	26.4 ± 2.0	1.042 ± 0.079
−0.550	25.0 ± 3.0	1.062 ± 0.128	24.2 ± 3.5	1.027 ± 0.147	24.5 ± 0.7	1.040 ± 0.032	20.0 ± 3.6	0.849 ± 0.154	27.2 ± 2.0	1.154 ± 0.087
−0.650	25.4 ± 3.2	1.137 ± 0.142	24.0 ± 3.6	1.076 ± 0.163	22.7 ± 0.7	1.020 ± 0.033	21.0 ± 3.8	0.940 ± 0.169	18.0 ± 1.8	0.808 ± 0.081
−0.750	21.8 ± 3.2	1.016 ± 0.149	16.1 ± 3.4	0.752 ± 0.159	22.5 ± 0.8	1.046 ± 0.038	27.0 ± 4.5	1.256 ± 0.208	20.9 ± 2.1	0.974 ± 0.097

Table 2: The differential Bhabha cross sections at energies of 14, 22, 34.8, 38.3, and 43.6 GeV. The scattering angle is given as central value of the correponding bin. The data points include statistical and systematic errors apart from an overall normalization uncertainty due to luminosity determination.

$\sin^2\theta_W$	0.24 ± 0.04
g_V^2	-0.08 ± 0.04
g_A^2	0.14 ± 0.09
Λ_+^{QED}	$> 435\,GeV$
Λ_-^{QED}	$> 590\,GeV$

Table 3: Results on electroweak parameters and lower limits (95% confidence level) on QED cut-off parameters Λ^{QED}. The errors given include statistical and systematic uncertainties.

Coupling	Λ_+^C (TeV)	Λ_-^C (TeV)
LL	1.4	3.3
RR	1.4	3.3
VV	3.6	7.1
AA	2.8	2.4

Table 4: Lower limits (95% confidence level) on mass scale parameters Λ^C in composite models for left handed (L), right handed (R), vector (V), and axial vector (A) couplings.

Figure captions

Figure 1. The differential Bhabha cross sections at energies of 14, 22, 34.8, 38.3, and 43.6 GeV. The curves show the QED predictions. The data points include statistical and systematic errors apart from an overall normalization uncertainty due to luminosity determination.

Figure 2. The differential Bhabha cross section normalized to the QED expectation for energies of a) $\sqrt{s} = 14\,GeV$, b) $\sqrt{s} = 22\,GeV$, c) $\sqrt{s} = 34.8\,GeV$, d) $\sqrt{s} = 38.3\,GeV$, and e) $\sqrt{s} = 46.8\,GeV$. The curves show the predictions of the standard model using $\sin^2\theta_W = 0.23$ and $M_Z = 92\,GeV$. The data points include statistical and systematic errors apart from an overall normalization uncertainty due to luminosity determination.

Figure 3. a) The total Bhabha cross section integrated over $|\cos\theta| < 0.8$ as function of the energy. The curve shows the QED prediction. b) The same data normalized to the QED prediction. The dotted curves show the expected deviations from QED for cut-off parameters of $\Lambda_+^{QED} = 370\,GeV$ and $\Lambda_-^{QED} = 190\,GeV$. The data points include statistical and systematic errors apart from an overall normalization uncertainty due to luminosity determination.

Figure 4. The differential Bhabha cross section normalized to the standard model expectation at $\sqrt{s} = 34.8\,GeV$. The curves show the possible contributions from compositeness for a) left handed or right handed coupling, b) vector coupling, and c) axial vector coupling. The data points include statistical and systematic errors apart from an overall normalization uncertainty due to luminosity determination.

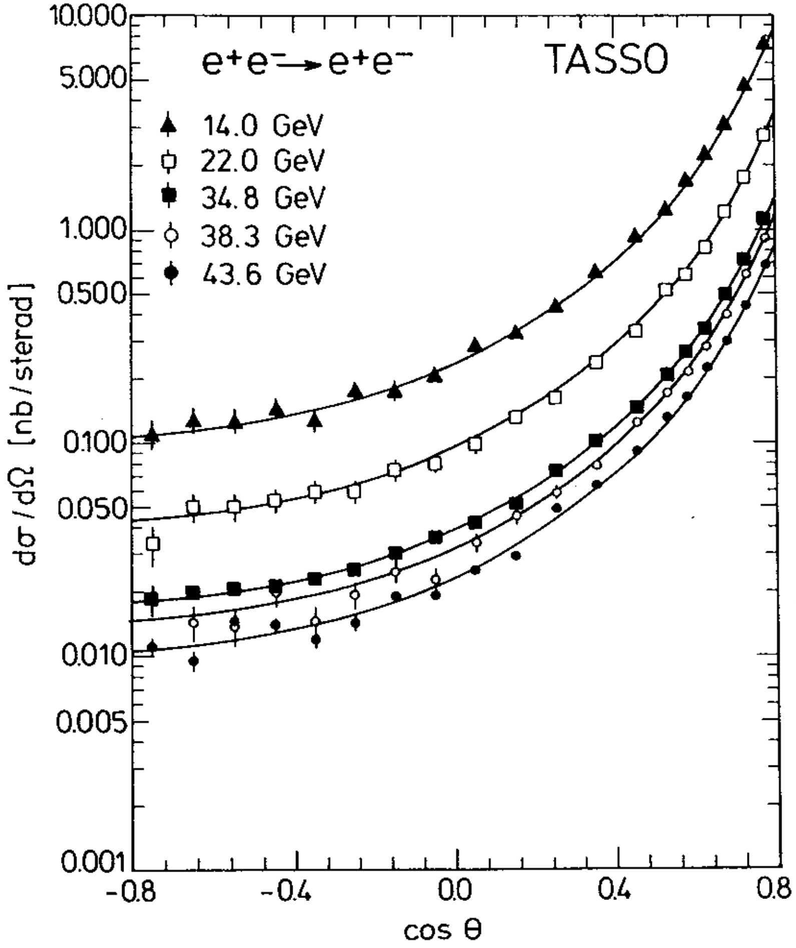

Fig. 1

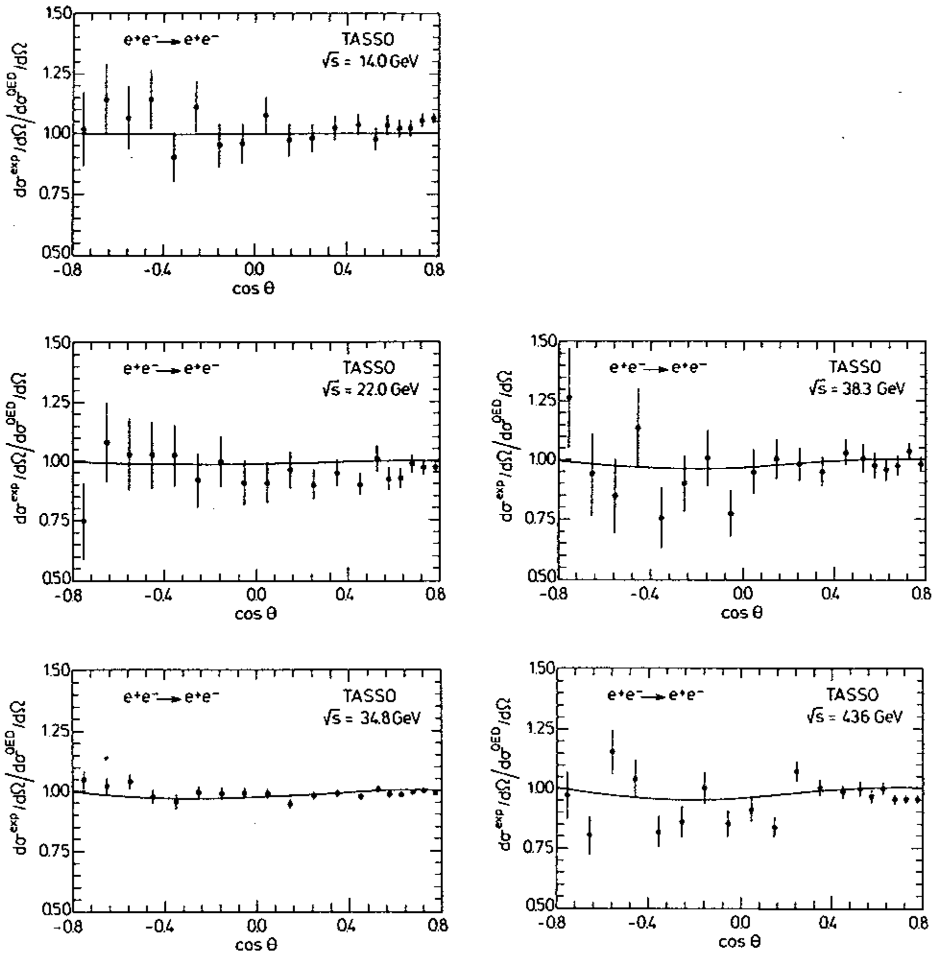

$e^+e^- \to e^+e^-$
TASSO
$\sqrt{s}$ = 14.0 GeV
$\sqrt{s}$ = 22.0 GeV
$\sqrt{s}$ = 38.3 GeV
$\sqrt{s}$ = 34.8 GeV
$\sqrt{s}$ = 43.6 GeV
$d\sigma^{exp}/d\Omega / d\sigma^{QED}/d\Omega$
$\cos\theta$

Fig. 2

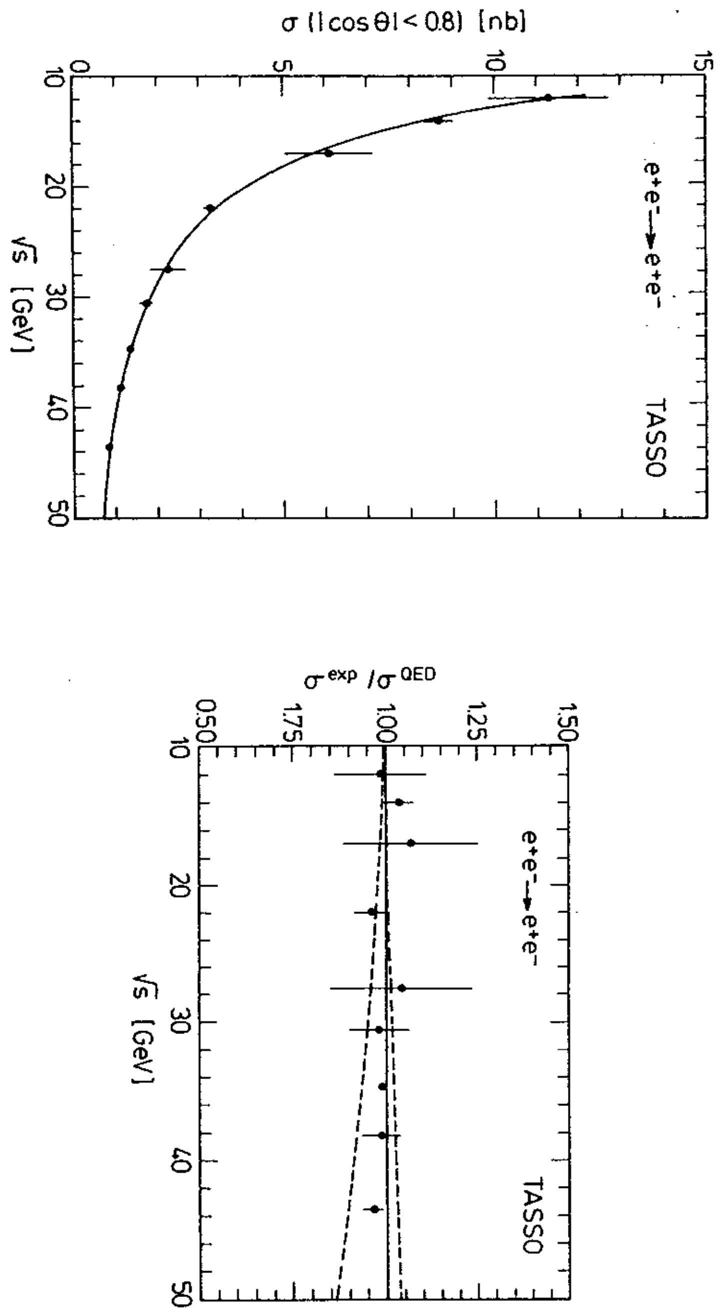

σ ($|\cos\theta| < 0.8$) [nb]
$e^+e^- \to e^+e^-$
TASSO
$\sqrt{s}$ [GeV]
$\sigma^{exp}/\sigma^{QED}$

Fig. 3

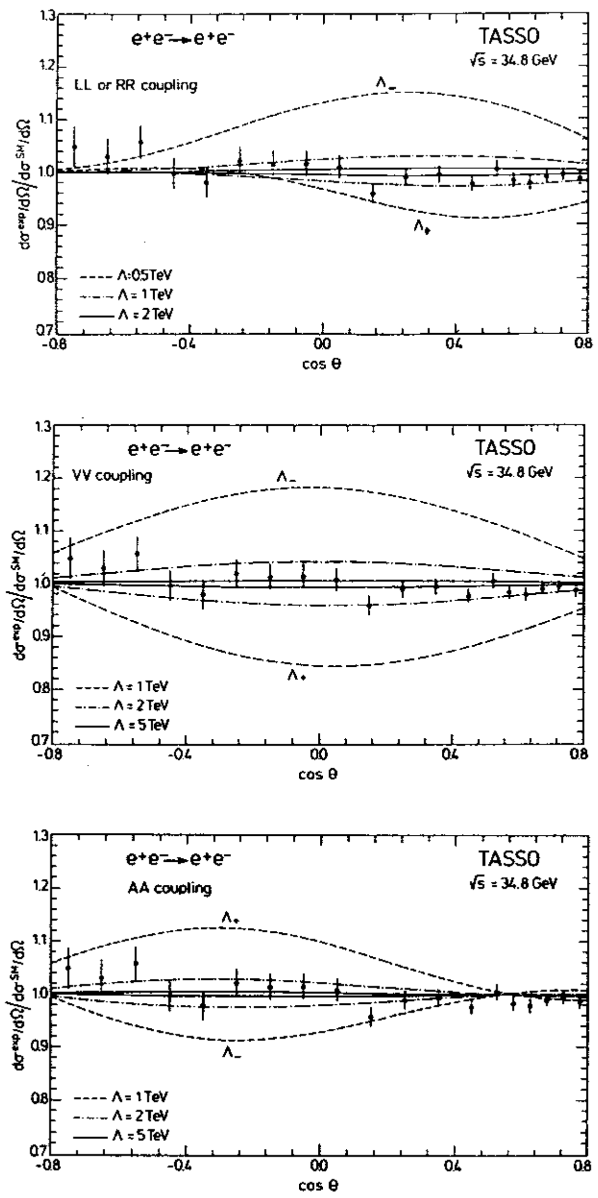

e+e- → e+e-
TASSO
√s = 34.8 GeV
LL or RR coupling
Λ-
Λ+
Λ=0.5 TeV
Λ = 1 TeV
Λ = 2 TeV
e+e- → e+e-
TASSO
√s = 34.8 GeV
VV coupling
Λ-
Λ+
Λ = 1 TeV
Λ = 2 TeV
Λ = 5 TeV
e+e- → e+e-
TASSO
√s = 34.8 GeV
AA coupling
Λ+
Λ-
Λ = 1 TeV
Λ = 2 TeV
Λ = 5 TeV
dσexp/dΩ/dσSM/dΩ
cos θ

Fig. 4